71st Conference of the Italian Thermal Machines Engineering Association, ATI2016, 14-16 September 2016, Turin, Italy

A simplified thermal model to control the energy fluxes and to improve the performance of buildings

Ludovico Danza[a]*, Lorenzo Belussi[a], Italo Meroni[a], Francesco Salamone[a], Fabio Floreani[b], Andrea Piccinini[b], Alberto Dabusti[c]

[a]Construction Technologies Institute, National Research Council of Italy (ITC-CNR), Via Lombardia, 49, 20098 San Giuliano Milanese (MI), Italy
[b]Consorzio Intellimech, Parco Scientifico tecnologico Kilometro Rosso via Stezzano, 87, 24126 Bergamo (BG), Italy
[c]Kofler Energies AG, Sickingenstraße, 39, 69126 Heidelberg, Germany

Abstract

The article describes an accurate and suitable simplified tool aimed at evaluating, controlling and managing heat energy fluxes in buildings. The focus is the development of a Resistance-Capacitance (RC) thermal model able to represent the envelope thermal inertia on an hourly time basis. The single RC module simulates the thermal response of a single opaque or transparent element of the envelope. Each module consists of 3 Resistances and 2 Capacitances and is connected to the other modules by thermal nodes and coupled to an air internal temperature node in order to obtain a realistic exemplification of the specific boundary conditions and gains distribution in the conditioned space. The differential balance equations in each node have been solved with an explicit numerical method using Modelica simulation tool. A monitoring campaign was carried out on an outdoor test cell in order to observe the real thermal dynamic behaviour and the real hourly energy needs. The results of the model have been compared with the experimental collected data. The results are presented in terms of temperatures and heating power hourly profiles and cumulative daily energy needs. Finally the Bland-Altmann plot has been used to verify the accuracy and the shortcomings of the proposed thermal model.

Keywords: Building energy simulation, lumped capacitance model, Bland-Altmann test, Co-heating test

---

* Corresponding author. Tel.: +39-029806424; fax: +39-0298280088.
  E-mail address: l.danza@itc.cnr.it

1. Introduction

Building Energy Simulation (BES) through numerical models is an area of active investigation [1, 2]. Significant effort has been spent to predict the energy demand of buildings and to evaluate their energy performance. Robust numerical methods are needed for a detailed mathematical description regarding a great number of variables needed to represent the user-building-environment interactions. The BES models are especially built to simulate existing or designed buildings and are applied in different ways so as to improve the efficiency of the building sector [2, 3]. Models are often embedded in control system in order to tune the controllers with the aim of predicting the building energy demand and optimizing the operating plants [4]. Alongside these models, the International Standards provide simplified methods, which should be realistic, sufficiently sensitive and robust but also reliable, verifiable, transparent and reproducible. Recent studies demonstrate the accuracy of these methods in building energy performance simulation [5] and the suitability in the development of control systems [6]. The BES model are classified into three categories, white, black and grey models according to the method applied for the resolution of the transient heat equations and the parameters used (physical, statistical or a combination of them, respectively) [7]. Among them, the grey box approaches use deterministic differential equations [8] and continuous time modelling to calibrate the parameters of the model on data [9]. It is a common approach to assemble simple thermal models [10]. The lumped capacitance grey-box models provide good results in terms of cost-effectiveness. They offer a good compromise between simplicity and computational expense. It is a well-recognized approach based on the analogy between thermal systems and electric circuits [11, 12]. The present article describes the development of a Resistance-Capacitance thermal model aimed at predicting the thermal behaviour of buildings [13, 14]. The reliability of the model has been assessed using the co-heating test, applied to a real test cell [15], and the results evaluated through the Bland-Altmann test [16]. The differential equations were solved implementing the model in Dymola, an object-oriented modeling language for large dynamical systems.

Nomenclature	
C	thermal capacity [J/K]
ϕ	thermal power [W]
H	heat transfer coefficient [W/K]
R	thermal resistance [W/K]
T	temperature [K]
A	area [m^2]
h	coefficient of heat transfer [W/m^2K]
I	irradiation [W/m^2]
t	time [hour]
σ	Stefan-Boltzmann's constant [W/m^2K^4]
λ	thermal conductivity [W/mK]
ε	emissivity [-]

Subscript	
air	air
i	internal
e	external
c	convection
set	set-point
s	surface
t	thermal
tr	transmission
o	overall
h	horizontal
H	heating
sol	solar radiation
w	window
in	inlet
out	outlet

2. Methodological approach

Equivalent Resistance-Capacitance (RC) schemes are broadly used to represent thermal systems. This method of representation derives from the lumped capacitance solution of the transient heat transfer equations: a well-known consequence of the thermal-electric analogy. A lumped model is based upon the assumption that the temperature of an element (or a part of it) is spatially uniform during a transient heat transfer. This is clearly not the case of the building envelope, where sparse temperature distributions come along with heat sinks (thermal bridges, air gaps etc.)

and gains (solar radiation etc.). Although this approach cannot represent a fine temperature distribution, it is a good candidate to represent the overall thermal behaviour of a building [17, 18, 19].

According to the lumped capacitance solution the heat balance equation acquires a first order differential layout and is capable to describe the evolving temperature of a thermal node T(t) [K] due to the storing Φ_{in} [W] and extraction Φ_{out} [W] of the heat power from the thermal mass of the system:

$$\frac{CdT(t)}{dt} = \Phi_{in} - \Phi_{out} \tag{1}$$

Considering a multi-layered wall, with an area A [m^2] equipped with an insulating coat (Fig. 1), it is possible to observe that the internal-external temperature gradient is considered the driving force for heat losses through the building envelope. This process could be represented, assuming a one-direction heat transfer through the building envelope, with two surface nodes, $T_{s,i}$ and $T_{s,e}$, linked through the thermal conductance, H_{tr} [W/K], which can be evaluated according to the materials features and construction techniques of the considered building element, as prescribed by EN ISO 13790 [20].
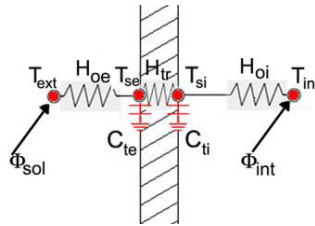

Fig. 1. Element heat balance and equivalent 3R2C module: a cross section temperature profile of a wall.

The thermal mass of the system stores and releases heat according to instantaneous boundary conditions – both defined from the internal space ($T_{s,i}$ node) and external environment ($T_{s,e}$ node). The external air temperature node, T_e, is a boundary condition; hence, a given profile of hourly temperature values is associated to it. This node is connected to the $T_{s,e}$ with an overall heat transfer coefficient, $H_{o,e}$ [W/K], representing the convective and radiative surface heat exchange altogether. The corresponding coefficient of heat transfer, $h_{o,e}$ [W/m^{2}K], can be evaluated with:

$$h_{o,e} = h_{c,e} + \sigma\varepsilon(T_{s,e} + T_e)(T_{s,e}^2 + T_e^2) \tag{2}$$

Similarly, it is possible to calculate the internal overall heat transfer coefficient, $H_{o,i}$. The resulting 3R2C thermal network is illustrated in Fig. 1. The balance equation of each node can be defined using the previously described quantities and applying the nodal potential method [21] to $T_{s,e}$ and $T_{s,i}$. Consequently, the surface heat balance can be defined for $T_{s,e}$ as follows:

$$C_{t,e} \frac{dT_{s,e}}{dt} = H_{o,e}(T_e - T_{s,e}) + H_{tr}(T_{s,i} - T_{s,e}) + \Phi \tag{3}$$

Where ϕ represents the sum of the thermal power in the internal environment (internal and solar heat). The heat flow through the wall depends on the surface temperatures differential. In the same way, a surface heat balance equation is defined for the internal surface node, $T_{s,i}$, connected to the thermal capacitance. As a consequence, the balance is described by a first order differential equation:

$$C_{t,i} \frac{dT_{s,i}}{dt} = H_{tr}(T_{s,e} - T_{s,i}) + H_{o,i}(T_i - T_{s,i}) + \Phi \tag{4}$$

Equations (3) and (4) lead to a first order differential equations system stated for each building component. Thus, a system of differential equations is defined for each module and describes the single building element thermal balance. Assuming to have *n* modules to describe a generic building, the i-th 3R2C module is connected to T_i and

heat flows, passing through it, reach all the others. The thermal network describing all the system is closed around this central node, where a heat balance can be defined, considering heat flows occurring in the internal space. By connecting each module with the others through the internal temperature node it is possible to determine the following balance equation:

$$C_{air}\frac{dT_i}{dt} = \sum_{i=1}^{n} H_{o,i}\left(T_{s,i_i} - T_i\right) + \Phi \tag{5}$$

With the modular 3R2C representation, the scheme maintains a simplified form and provides a spatial description of the analyzed space. This special feature allows to localize heat gains in a specific position in the modelled space. On the other hand the modules are linked to each other through the T_i central node, inter-elements conductive heat flows are therefore neglected. Solar radiation enters through the glazing and produces a solar gain. The heated floor charges the building thermal mass and introduces an important phase shift to the energy demand delivered to maintain a set-point temperature. The radiated area on the floor and the hourly view factor are calculated as functions of the sun-floor relative position. For each hour a value of $\phi_{sol,w}$ is calculated. Then the heat output of the heater Φ_H is calculated, according to the current heating schedule (on/off) and value of $T_{set,H}$, with the following relation:

$$\Phi_H = \sum_{i=1}^{n} H_{o,i_i}\left(T_{set,H} - T_i\right) \tag{6}$$

The value of Φ_H is limited to the maximum power output of the heater: $0 < \Phi_H < 2$ kW. It is assumed that the heater has a thermal efficiency close to 1, therefore 2 kW is the maximum energy output. Air changes measurements into the air extraction pipe have been performed, consequently 35 m³/h airflow has been estimated to represent the overall infiltration and ventilation rate. This value is constant within the considered interval.

The model, described by an implicit system of Differential/Algebraic Equations (DAE), has been solved by means of DASSL [22], a variable step solver. DASSL solver uses backward differentiation formulas to integrate DAE. In particular Dymola is an object-oriented modeling language for modeling of large dynamical systems [23]. Dymola works implementing the Backwards Differentiation Formulas (BDF) from order one to five. BDF are linear multistep methods which approximate the derivative of a function taking data from previous time iterations reducing uncertainty introduced by the last approximation.

3. Case study

In order to test the model, an external test cell located at ITC-CNR headquarters near Milan was used. The test building is a single-space test cell (dimensions 2.8 m x 5 m x 2.8 m) with a concrete frame external envelope and a slab-on-ground foundation and was equipped with the necessary devices to perform a co-heating test. The outer layer of the envelope is a 0.12 m insulating coating of polystyrene light foam ($\lambda = 0.032$ W/mK). The floor is insulated with a 0.24 m insulation layer. The South-facing short side is a wall of polystyrene equipped with a low-E glazing ($\epsilon = 0.25$) element (dimensions 1.9 m x 1.5 m). The other sides are walls of concrete insulated on the outside. The electric heater is controlled through a differential thermostat with a ±0.5 °C threshold around the set-point temperature, in intermittent heating mode. The heater works from 7am to 6pm every day of the week with 20 °C set-point temperature and is switched off during the weekend. A long switch off has been performed in order to show a long cooling down transient phase and an analogous long heating phase. The collection of these data allows to evaluate the thermal lag, introduced by the heavyweight elements. A first monitoring campaign was performed on the cell during the winter season (October 2013 - March 2014). The cell is conditioned with a 2 kW high efficient electric heater placed in the center of the space. An air extractor located in the north wall provides the space ventilation (1 air change per hour) while a ceiling fan mixes the air. To undergo a thorough metering, the cell is equipped with Pt100 contact temperature sensors with four wires on the internal surfaces in the sheltered air volume. Furthermore, the energy output from the heater has been detected. A weather station, located close to the cell, detects external air temperature, T_e [°C], and global horizontal irradiation values, I_h [W/m²]. The envelope of the cell has been split (Fig. 2) into 7 elements: 1 roof, 4 walls (North, South, West and East), 1 floor and 1 glazing. Even though

the glazing is included in the South wall, a window module has been created in order to compare calculated and measured glass surface temperature profiles. T_e hourly profile, detected by the weather station, represents the external boundary condition of all the 3R2C modules. Once assembled the model and defined the boundary conditions, the parameters characterizing each module have been calculated according to the standards calculation procedures and hourly inputs (heat gains/losses and plant settings) have been defined. The heat balance of each module is described by equations (3) and (4) and then equation (5) defines the thermal zone air heat balance.
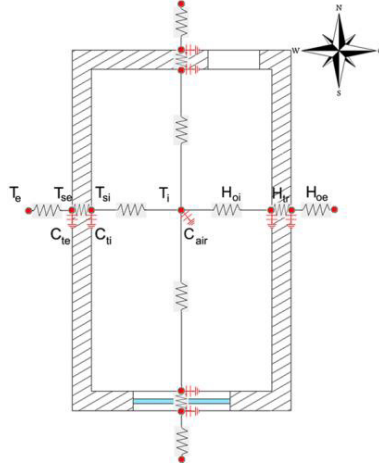

Fig. 2. Coupling of the 3R2C modules of the test cell

4. Discussion and Results

Calculation results are hourly profiles of surface temperatures, $T_{s,i}$ and $T_{s,e}$, of each considered 3R2C module. Results relative to a representative period are showed in the following figures, in order to analyze the features of the developed model. In Fig. 3 the results related to South Walls for a week in November are plotted: the calculated (red line) and measured (green line) hourly values of $T_{s,i}$ are illustrated along with the measured T_e (black line).

Note that each calculated $T_{s,i}$ profile exhibits a particular dynamic response. T_e fluctuations passing through the envelope are in fact damped and shifted in time, according to materials thermo-physical features. The $T_{s,i}$ calculated profile shows a remarkable accuracy to related measures and it exhibits typical non-linear trends giving an inertial description of temperature evolution. The comparison between $T_{s,i}$ profiles in Fig. 3 shows how the measured and calculated patterns are similar and both disturbed by weather temperature fluctuation, due to lower $C_{t,i}$ of window.
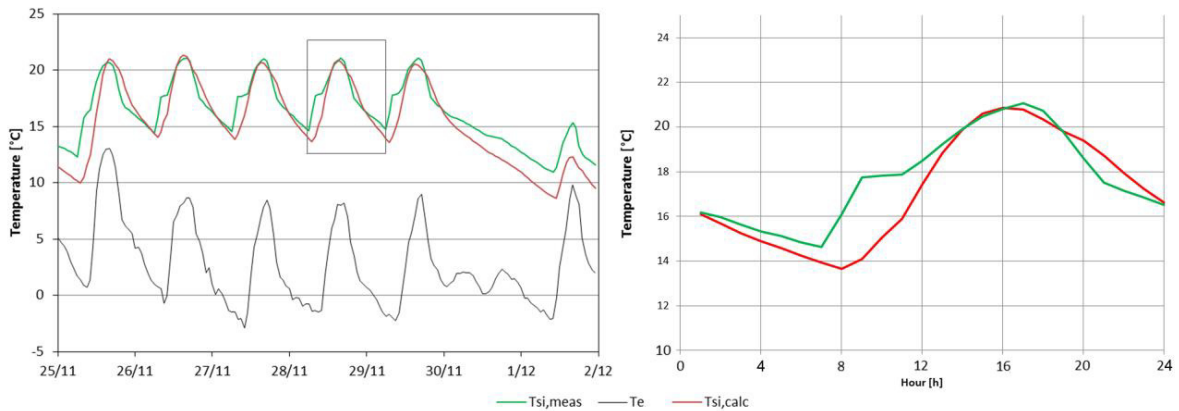

Fig. 3. South Wall: comparison between measured and calculated temperatures

The monitoring campaign has been performed on the examined test building in order to compare these values with the results of the calculation on an hourly basis. Fig. 4 shows hourly series of calculated and measured T_i and Φ_H along with measured T_e, which shows the weather influence on the main variables.
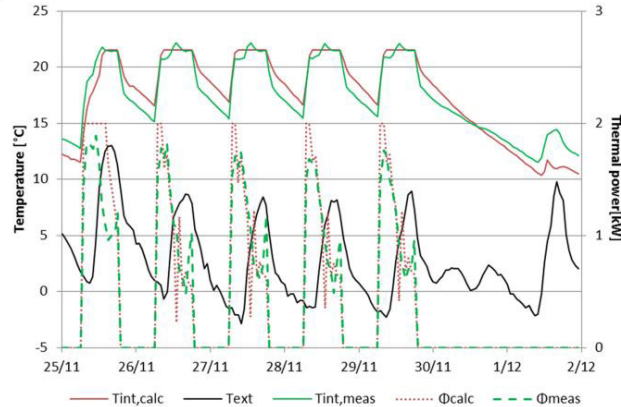

Fig. 4. Comparison between calculated and measured internal air temperatures and energy powers

Remarkable differences between simulations and measurements occur on the first day of the week after a switch off of the heating plant. If the calculation results show that the T_i is close to the set-point ($\approx 21°C$), the measured ones reach these values in the morning after few hours. As a consequence the calculated energy output (red) is slightly overestimated. In particular, the model predicts that on Monday 25th the plant is working at maximum power (2 kW), although measured data show that this value is not reached. Similarly, every day at 7am the measured power is maximum with respect to the calculated ones. These first results show that the thermal inertia of the envelope has been overestimated: a positive outcome for the energy needs prediction. The calculated heat power values maintain generally a "zig-zag" profile in time and exhibit peaks in the first heating hour. Measured T_i profile exhibits daytime peaks, when solar gains are at the edge according to the hourly daylighting conditions. The increases of I_h and T_e induce an energy dropdown, a trend particularly remarkable when solar gains are at the maximum. As a consequence of the resolution method the fluctuation in energy need is less intense on measured Φ_H profile. Φ_H is calculated with regard to T_i values under the hypothesis of a previous hour switch off. Due to the length of the time step and to the heat capacity of the internal air temperature node, quick variations of internal air temperature are not presented. Hence, an intermittent power release is produced. Nevertheless, the hourly energy consumption can be aggregated on longer and more descriptive time patterns (e.g. weekly, monthly energy consumption). At the end of the whole monitoring period, cumulated energy needs are 2.7 % higher than measured, hence it can be stated that the method is conservative on this time span.

Although the previous profiles show the accuracy obtained by the 3R2C module, the internal air temperature T_i and space-heating hourly needs Φ_H are the most important variables to assess the thermal and energy performances of the test building. The Bland-Altmann plot [16] is used in order to analyze the consistency between calculated and measured values of T_i and Φ_H. As prescribed by Bland et al. the plot is formed by displaying the average (X) of the paired values from each method on the x-axis and the difference (d) between them on the y-axis. The bias, the central line on the B.A. plot, defines the average of the difference values and it quantifies to what extent the new method over or underestimates the state variable, compared to the reference data measured. The Standard Deviation (SD) of all individual differences defines the upper and the lower Limit of Agreement (LoA). The 95% (Mean difference $\pm$ 1.96 SD) and 99.7% ($\pm$ 3 SD) confidence limits are used to verify if the sample displays a normal distribution. When the % of values within the LOAs is close to the above stated percentages the difference is Gaussian-wise distributed, hence a high agreement between the methods occurs. Results of the methodology are given in Bland-Altmann plots (Fig. 5) regarding Φ_H. Results reported in Table 1 show that the model gives a better prediction of the T_i measured values than energy consumption, because the percentages of inliers related to T_i are closer to the normal distribution values. Results in terms of bias values referred to the considered time span, show

that the model overestimates the plant energy output Φ_H for 12.7 Wh, while it underestimates the internal temperature T_i for -0.08 K.

Table 1 - Consistency verifications of model values and experimental results

Indices	Average Differences between Calculated and Experimental values $\overline{x}$	Average Standard Deviations between Calculated and Experimental values s	The 95% Confidence Interval	The 99% Confidence Interval
Energy consumption	12.7 Wh	208 Wh	91.71 %	97.41 %
Internal air temperature	-0.08 K	1.28 °C	94.52 %	99.23 %

Note that differences are mainly scattered around the bias, some values and outliers draw a line, which indicates that the ratio of the difference on the mean is constant for all these values. This particular correlation can be explained if power output hourly profiles are considered. According to model results, the plant met the maximum power output every first hour during heated days of the colder months, although metered values show this is not happening. Differences between calculated and actual power output are really high in these hours, and the upper value is always the constant maximum heater power (2 kW).
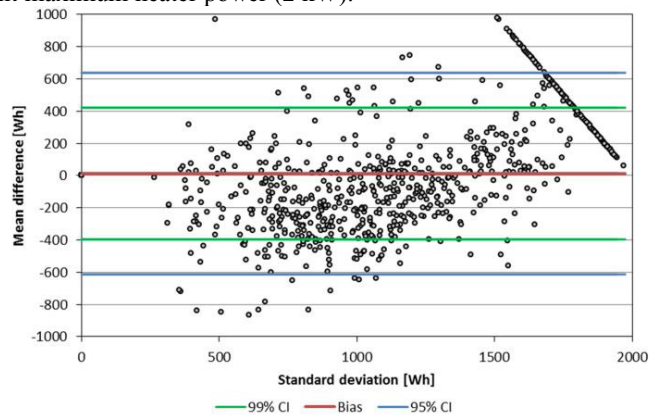

Fig. 5. Bland-Altmann plot: energy consumption of the whole experimentation

5. Conclusions

The present work focuses on the idea of using the lumped solution's uttermost important features - modularity - to build a 3R2C module suitable for the representation of heat gains, losses and dynamic response of a single element of the building envelope. The idea is to make a state space representation of the building envelope that allows to give a physical meaning to system's parameters and boundary conditions. The 3R2C module is the basic constituent of the model and a method to divide the building shell into components is described. A whole system RC scheme is then assembled, connecting these modules according to the structure of the building envelope, through the internal air temperature node. The presented procedure could be a feasible way to speed up the modelling phase and to obtain a simple physical representation of the system. A balance equation on the internal air temperature node allows to assess the internal space conditions and each module plays the role of weighting factor. Hence, the internal temperature is determined by means of surface temperature values as for the operative temperature, which describes internal conditions according to surfaces radiative and convective heat exchange. Results obtained for the investigated test cell are compared with the hourly profiles of the measured data. The comparison shows a remarkable consistency between results and measured data. Both internal surface and air temperature exhibit a dynamic evolution, determined from internal space use conditions and weather variables. Each module shows its specific inertial behaviour, according to its thermo-physical features. It shows a realistic response to solar gains. The overall energy needs, calculated for the analyzed time span is 2.7% higher than the metered ones. The model results exhibit in general a greater inertia: the heat exchange is slower than the measured values. This slow response can be

imputed to the model layout: the internal air temperature is the only connection between modules and that is clearly a strong approximation. In fact the internal air temperature node is directly interconnected with the adjacent building components. The simplified model leads to different applications. On the one hand, the model allows to assess different operational scenarios that could be compared in order to give a practical answer about how to manage the envelope in order to obtain a higher performance level. On the other hand, the method can be proposed to increase the energy efficiency or thermal comfort of buildings by comparing energy consumption and PMV values scenarios according to particular design solutions and operational conditions, i.e. the minimum acceptable PPD index and the switch on time of the plant [24, 25]. Once validated, these information - along with input profiles - help to understand the system thermal behaviour and inefficiencies due to a faulty design or incorrect user behaviour.

References

[1] Coakley, D., Raftery, P., & Keane, M. (2014). A review of methods to match building energy simulation models to measured data. Renewable and Sustainable Energy Reviews, 37, 123-141.

[2] Belussi, L., Danza, L., Meroni, I., Salamone, F., Ragazzi, F., Mililli, M. (2013). Energy performance of buildings: A study of the differences between assessment methods. In Energy Consumption: Impacts of Human Activity, Current and Future Challenges, Environmental and Socio-Economic Effects; Nova Science Publishers: New York, NY, USA.

[3] Belussi, L.; Danza, L.; Meroni, I.; Salamone, F. Energy performance assessment with empirical methods: application of energy signature. Opto-Electronics Review 2015, 23, 1, 85-89.

[4] Harish, V. S. K. V., & Kumar, A. (2016). A review on modeling and simulation of building energy systems. Renewable and Sustainable Energy Reviews, 56, 1272-1292.

[5] Kircher, K. J., & Zhang, K. M. (2015). On the lumped capacitance approximation accuracy in RC network building models. Energy and Buildings, 108, 454-462.

[6] Chen, X., Wang, Q., & Srebric, J. (2015). Model predictive control for indoor thermal comfort and energy optimization using occupant feedback. Energy and Buildings, 102, 357-369.

[7] Amara, F., Agbossou, K., Cardenas, A., Dubé, Y., & Kelouwani, S. (2015). Comparison and simulation of building thermal models for effective energy management. Smart Grid and Renewable Energy, 6(4), 95.

[8] Andersen, K. K., Madsen, H., & Hansen, L. H. (2000). Modelling the heat dynamics of a building using stochastic differential equations. Energy and Buildings, 31(1), 13-24.

[9] Bacher, P., Madsen, H. (2011). Identifying suitable models for the heat dynamics of buildings. Energy and Buildings, 43(7), 1511-1522.

[10] O'Brien, W. (2015). Modeling, design, and optimization of net-zero energy buildings. A. K. Athienitis (Ed.). Ernst, Wilhelm & Sohn.

[11] Evangelisti, L., Guattari, C., Gori, P. (2015). Energy Retrofit Strategies for Residential Building Envelope: An Italian Case Study of an early-50s Building, Sustainability, 7(8), 10445-10460.

[12] Davies, M. G. (1983). Optimum design of resistance and capacitance elements in modelling a sinusoidally excited building wall, Build. Environ. 18, 19-37.

[13] Nielsen, T. R. (2005). Simple tool to evaluate energy demand and indoor environment in the early stages of building design. Solar Energy, 78(1), 73-83.

[14] Fraisse, G., Viardot, C., Lafabrie, O., & Achard, G. (2002). Development of a simplified and accurate building model based on electrical analogy. Energy and buildings, 34(10), 1017-1031.

[15] Bauwens, G., & Roels, S. (2014). Co-heating test: A state-of-the-art. Energy and Buildings, 82, 163-172.

[16] Bland, J. M., & Altman, D. G. (2010). Statistical methods for assessing agreement between two methods of clinical measurement. International Journal of Nursing Studies, 47(8), 931-936.

[17] Dimitriou, V., Firth, S. K., Hassan, T. M., Kane, T., & Fouchal, F. (2014). Developing suitable thermal models for domestic buildings with Smart Home equipment.

[18] Nespoli, L., Medici, V., & Rudel, R. Grey-box system identification of building thermal dynamics using only smart meter and air temperature data.

[19] Danza, L., Belussi, L., Meroni, I., Mililli, M., & Salamone, F. (2016). Hourly Calculation Method of Air Source Heat Pump Behavior. Buildings, 6(2), 16.

[20] ISO, E. (2008). 13790: 2008. Energy performance of buildings–Calculation of energy use for space heating and cooling.

[21] Michalak, P. (2014). The simple hourly method of EN ISO 13790 standard in Matlab/Simulink: A comparative study for the climatic conditions of Poland. Energy, 75, 568-578.

[22] Petzold, L. R. (1982). A description of DASSL: A differential/algebraic system solver. Scientific computing, 1.

[23] Otter, M., Elmqvist, H., & Cellier, F. E. (1996). Modeling of multibody systems with the object-oriented modeling language Dymola. Nonlinear Dynamics, 9(1-2), 91-112.

[24] Salamone, F.; Belussi, L.; Danza, L.; Ghellere, M.; Meroni, I. Design and Development of nEMoS, an All-in-One, Low-Cost, Web-Connected and 3D-Printed Device for Environmental Analysis. Sensors 2015, 15, 13012–13027.

[25] Salamone, F.; Belussi, L.; Danza, L.; Ghellere, M.; Meroni, I. An Open Source "Smart Lamp" for the Optimization of Plant Systems and Thermal Comfort of Offices. Sensors 2016, 16, doi:10.3390/s16030338.